Journal of Korean Association of Crystal Growth
Vol. 8, No. 1 (1998) 117-123

Evaluation of mechanical backside damage by minority carrier recombination lifetime and photo-acoustic displacement method in silicon wafer

Chi Young Choi and Sang Hee Cho
Department of Inorganic Materials Engineering, Kyungpook National University, Taegu 702-701 Korea

실리콘 웨이퍼에서 광열 변위법과 소수 반송자 재결합 수명 측정에 의한 기계적 후면 손상 평가

최치영, 조상희
경북대학교 무기재료공학과, 대구, 702-701

Abstract We investigated the effect of mechanical backside damage in Czochralski grown silicon wafer. The intensity of mechanical damage was evaluated by minority carrier recombination lifetime by laser excitation/microwave reflection photoconductivity decay method, photo-acoustic displacement method, X-ray section topography, and wet oxidation/preferential etching methods. The data indicate that the higher the mechanical damage intensity, the lower the minority carrier lifetime, and the photo-acoustic displacement values increased proportionally, and it was at Grade 1:Grade 2:Grade 3 = 1:19.6:41 that the normalized relative quantization ratio of excess photo-acoustic displacement in damaged wafer was calculated, which are normalized to the excess PAD from sample Grade 1.

요 약 초크랄스키 실리콘 기판의 뒷면에 형성된 기계적 손상이 미치는 효과에 대하여 고찰하였다. 기계적 손상의 정도는 레이저 여기/극초단파 반사 광전도 감쇠법에 의한 소수반송자 재결합 수명, 광열 변위, X-선 단면 측정 및 습식산화 /선택적 식각 방법으로 평가하였다. 그 결과, 웨이퍼 뒷면에 가해지는 기계적 손상의 세기가 강할수록 소수반송자 재결합 수명은 짧아지고, 광열 변위의 평균값은 비례적으로 증가하였으며, 손상된 웨이퍼에서 Grade 1의 과잉 광

열 변위 값을 1로 봤을 때 과잉 광열 변위의 정규화한 상대 정량 비는 Grade 1:Grade 2: Grade 3 = 1:19.6:41이다.

1. Introduction

It has been reported [1,2] that laser excitation / microwave reflection photoconductivity decay (μ-PCD) method is a noncontact, nondestructive, and high throughput technique with higher sensitivity than secondary ion mass spectroscopy and total reflection X-ray fluorescence spectrometry in metal contamination monitoring point of view. Also it is commonly recognized that minority carrier lifetime measured by μ-PCD method is very sensitive to crystallographic defects which can act as trap centers [3]. The other technique, that is, photo-acoustic displacement (PAD) method, is applicable to the monitoring of low-level lattice damage in the manufacturing processes of VLSI.

In silicon wafer industry, mechanical damage method, which provides dislocation and/or stacking fault nuclei [4,5] on wafer backside, is one of the extensively used extrinsic gettering techniques [6] since it is simple and less costly.

In this work, various experimental evaluations on the effect of mechanical damage of backside in Czochralski (CZ) silicon wafers was executed by μ-PCD method, PAD technique, X-ray section topography, and wet oxidation/preferential etching methods.

2. Experimental

The starting materials in this study were p-type (boron-doped, 9-20 $\Omega \cdot$ cm) CZ silicon wafers, with 200 mm diameter (100), single-side polished, and 725 μm thick. The oxygen concentration measured with Bio-RAD QS-300 FTIR according to the New ASTM procedure (ASTM F121-81 [7]) was 13.3~16.6 ppma, whereas the carbon level was less than 0.05 ppma which is below the detection limit of FTIR.

The wafers were heat treated at 700℃ for 10 min in N_2 ambient for oxygen donor annihilation [8] and each cleaved into quarter pieces. One piece from each wafer was not mechanically damaged. This piece was designated as reference to distinguish it from the second, the third and the fourth pieces, designated Grade 1, Grade 2, and Grade 3, whose backsides were mechanically damaged with three

Table 1
Liquid honing process parameters

Grade	Air pressure* (kgf/cm^2)	Conveuer speed* (mm/sec)	No. of npzzle*
1	1	12.3	1
2	4.3	12.3	1
3	5.7	10	2

(* : normalized value)

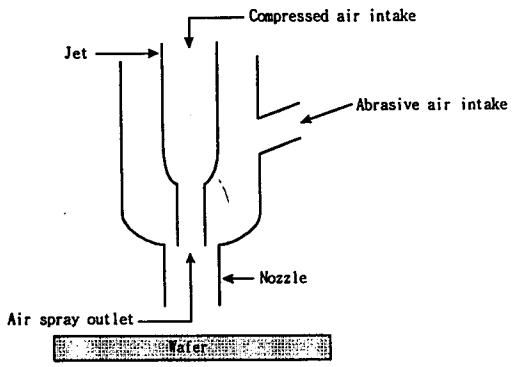

Fig. 1. Schematic of liquid honing method.

kinds of grades as shown in Table 1, respectively, using liquid honing method (in Fig. 1).

After liquid honing process, the samples were cleaned by RCA cleaning method and then subjected to surface passivation treatments, such as HF dipping for 10 min by high purity 49 % HF chemical of semiconductor grade and dry oxidation at 1000℃ for 40 min (the thickness of grown oxide layer is about 400 Å), to minimize the surface recombination velocity for lifetime measurements [9].

The measurement of minority carrier recombination lifetime for the samples was performed at room temperature with μ-PCD lifetime measurement system (SEMILAB WT-85X). The decay of excess minority carriers generated by irradiation with a pulsed laser beam (pulse width : 200 nsec, wavelength : 904 nm) impinged onto the polished surface is observed by monitoring the time decay of the microwave (10 GHz) reflection power since the conductivity decreases with the recombination of excited carriers and accordingly the microwave reflection power decays.

The stresses on as-received wafers caused by mechanical damage were evaluated by employing PAD method (PA 300 model) and X-ray topography system (Bede L6). In order to reveal the defects generated as a result of relieving the stresses caused by liquid honing method, the samples were oxidized at 1100℃ for 60 min in wet oxygen ambient and then inspected under the optical microscope after Wright etching [10] for 1 min.

3. Results and discussion

3.1. Relationship between mechanical damage intensity and lifetime

Figures 2(a) and (b) shows minority carrier recombination lifetime data measured with μ-PCD technique in nondamaged ("Reference") and backside mechanically damaged silicon wafers. These data clearly show that the higher the mechanical damage intensity, the lower the minority carrier lifetime. It is well known that the actual penetration depth of laser beam (904 nm wavelength) into silicon crystal bulk is less than 30 μm [11].

However, as shown in Fig. 2, it is obvious that electrons and holes excited by laser beam are propagated up to wafer backside, consequently affecting the minority carrier recombination lifetime value. Judging from this, we can suggest that

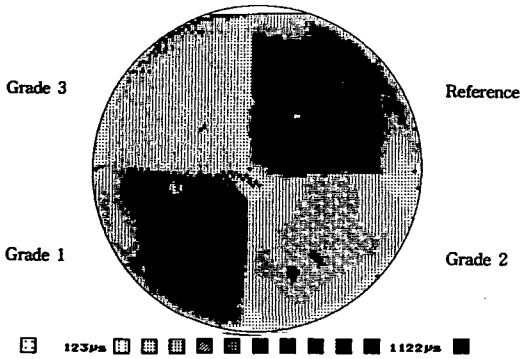

Reference	Grade 1	Grade 2	Grade 3
894.4	846	233.1	158.8

[μs]

(a) Lifetime mapping data and average values

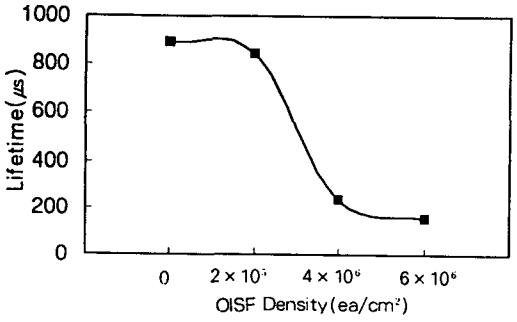

(b) Trend of average lifetime values

Fig. 2. Relationship between mechanical damage intensity and minoriy carrier recombination lifetime measured by μ-PCD technique. (a) Lifetime mapping data and average values and (b) Trend of average lifetime values.

nondamaged wafers be used to obtain correct data for contamination and defect monitoring during device processing.

3.2. Characterization of Stresses

To evaluate the stresses caused by liquid honing method, we have performed PAD and X-ray section topography analyses. The PAD technique is based on the sensitive measurements of the surface displacement due to the absorption of laser-light energy. The PAD simply depends upon the ratio of the thermal expansion coefficient to the thermal conductivity (κ) for a homogeneous sample. κ is strongly dependent on the crystal structure. Since lattice defects cause κ to decrease, we expect PAD to increase with the amount and extent of defects present in materials. It is of course true that change in κ is determined by the total amount of defects within the range of interaction of the thermal wave [12]. Generally, the PAD is very small (less than 1000 pm). It means the unit of photoacoustic displacement amplitude, and 1 PAD is equal to 0.1 pm, equivalent to the sensitivity of PAD measrement [13]. Figure 3 shows PAD values increased with the mechanical damage intensity. These data correspond to the result of damage formed by ion implantation [14]. Average PAD values of each grade are as follows; 118 in Reference, 128.2 in Grade 1, 317.6 in Grade 2, 535.8 in Grade 3 each. Reference wafer is highly perfect and strain free near the surface, that is, excess PAD value is zero. In case of damaged wafers (Grade 1,2,3), we are able to refer to including excess PAD values. We can also find out that the normalized relative quantization ratio of excess PAD is Grade 1: Grade 2:Grade 3 = 1:19.6:41, which are

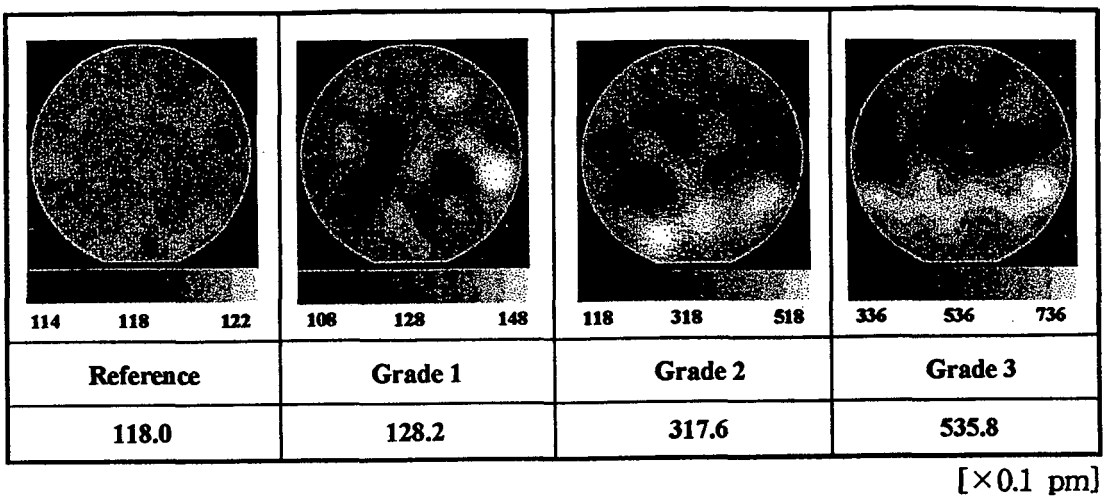

(a) PAD mapping data and average values

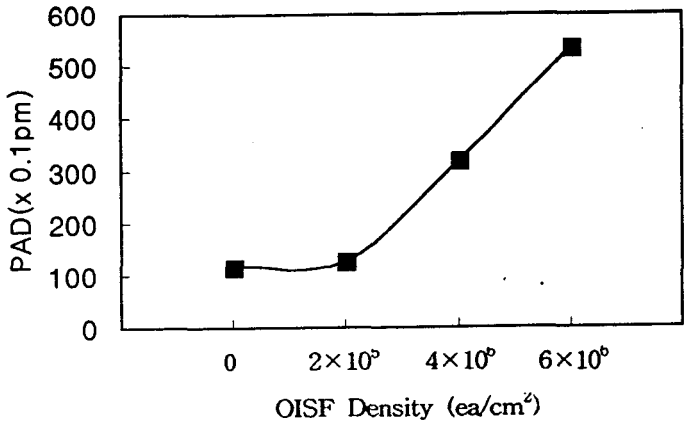

(b) Trend of average PAD values

Fig. 3. Relationship between mechanical damage intensity and PAD value. (a) PAD mapping data and average values and (b) Trend of average PAD values.

normalized to the excess PAD from sample Grade 1.

Figure 4 displays the stresses revealed by X-ray section topography technique with (440) reflection and Mo $K\alpha_1$. The Pendellösung fringes indicate high perfection of CZ silicon wafers used for this study. These data clearly indicate that the stresses even in Grade 1 of liquid honing method are propagated from mechanically damaged points on backside toward front surface to the extent of almost whole wafer thickness.

The defects on the front side of the samples generated during wet oxidation at 1100℃ for 60 min as a result of relieving

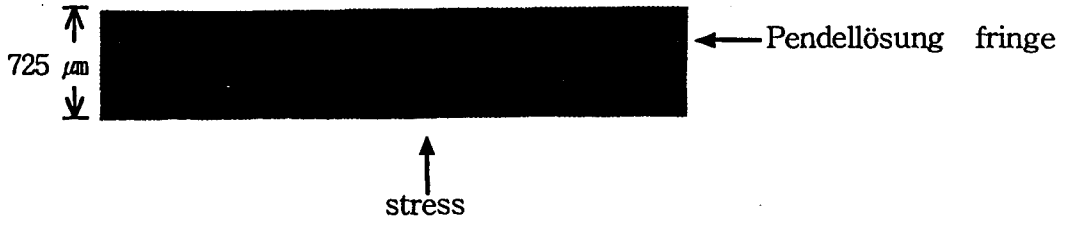

Fig. 4. The stresses reveaed by X-ray section topograph. [(440) reflection, Mo $K\alpha_1$]

the stresses caused by liquid honing method are shown in Fig. 5, and the data as follows ; Grade 1 is 2×10^5 ea/cm^2, Grade 2 is 4×10^6 ea/cm^2, Grade 3 is 6×10^6 ea/cm^2 each. Note that the harder the mechanical damage intensity, the higher the oxidation induced stacking fault (OISF) density. It can be deduced that OISF test method would be a useful way to distinguish mechanical damage grades.

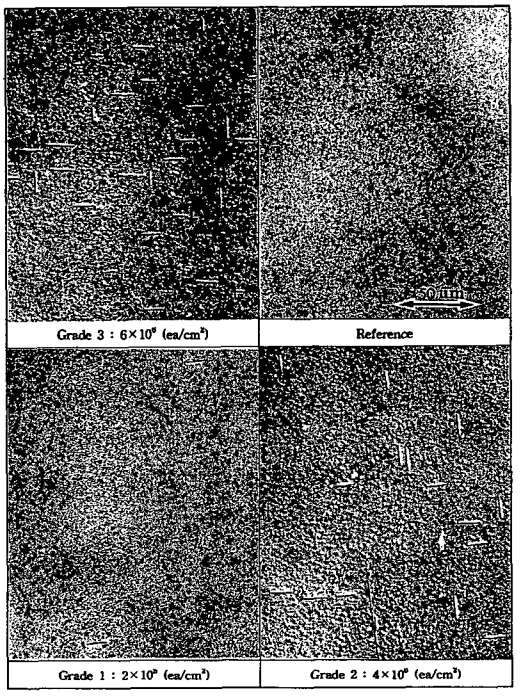

Fig. 5. Oxidation induced stacking faults generated during wet oxidation at 1100℃ for 60 min.

4. Conclusions

The stresses caused by mechanical damage and their effects were evaluated by minority carrier recombination lifetime by laser excitation/microwave reflection photoconductivity decay method and photo-acoustic displacement method, X-ray section topography, and wet oxidation/preferential etching methods.

The results indicate that :

1) The higher the mechanical damage intensity, the lower the minority carrier recombination lifetime,

2) The photo-acoustic displacement values increased proportionally, and the normalized relative quantization ratio of excess PAD is Grade 1:Grade 2:Grade 3 = 1:19.6:41, which are normalized to the excess PAD from sample Grade 1.

References

[1] A. Usami, Proc. IEEE 1991 Int. Conference on Microelectronic Test Structures 4 (1991) 25.

[2] A. Buczkowski, Z.J. Radzimski, G. A. Rozgonyi, and F. Shimura, J. Appl. Phys. 72 (1992) 2873.

[3] K. Katayama, Y. Kirino, K. Iba and F. Shimura, Jpn. J. Appl. Phys. 30 (1991) L1907.

[4] M.L. Polignano, G.F. Cerofolini, H. Bender and C. Claeys, J. Appl. Phys. 64 (1988) 869.

[5] F. Shimura, Semiconductor silicon crystal technology, (Academic Press, Inc., San Diego, 1989) p.350.

[6] S. Hahn, 1989 International Conference on VLSI and CAD, (KITE/ IEEE Korea section) 238.

[7] Annual Book of ASTM Standards, F121-81, (American Society for Testing and Materials, Philadelphia, 1987).

[8] V. Cazcarra and P. Zunino, J. Appl. Phys. 51 (1980) 4206.

[9] D.K. Schroder, Semiconductor material and device characterization, (John Wiley & Sons, Inc., New York, 1990) p. 359.

[10] M.W. Jenkins, J. Electrochem. Soc. 124 (1977) 757

[11] B. Braunstein et al., Phys. Rev. 107 (1958) 675.

[12] S. Sumie, H. Takamatsu and T. Nishino, Defect and Diffusion Forum Vols. 115-116, (Scitec Publications, Switzerland,1994) p. 85.

[13] S. Sumie, H. Takamatsu, Y. Nishimoto, T. Horiuchi, H. Nakayama, T. Kanata and T. Nishino, Jpn. J. Appl. Phys. 31 (1992) 3575.

[14] G. Washidzu, T. Hara, R. Ichikawa, H. Takamatsu, S. Sumie, Y. Nishimoto, Y. Nakai, H. Hashizume and T. Miyoshi, Jpn. J. Appl. Phys. 30 (1991) L1025.